Spin polarization of electrons with Rashba double-refraction

2004 J. Phys.: Condens. Matter 16 9143

(http://iopscience.iop.org/0953-8984/16/50/005)

INSTITUTE OF PHYSICS PUBLISHING JOURNAL OF PHYSICS: CONDENSED MATTER

J. Phys.: Condens. Matter **16** (2004) 9143–9154 PII: S0953-8984(04)83810-4

Spin polarization of electrons with Rashba double-refraction

V Marigliano Ramaglia, D Bercioux[1], V Cataudella, G De Filippis and C A Perroni

Coherentia-INFM and Dipartimento di Scienze Fisiche Università degli Studi Federico II, Napoli, I-80126, Italy

Received 8 July 2004, in final form 8 November 2004
Published 3 December 2004
Online at stacks.iop.org/JPhysCM/16/9143
doi:10.1088/0953-8984/16/50/005

Abstract
We demonstrate how the Rashba spin–orbit coupling in semiconductor heterostructures can produce and control a spin-polarized current without ferromagnetic leads. The key idea is to use spin-double refraction of an electronic beam with a nonzero incidence angle. A region where the spin–orbit coupling is present separates the source and the drain without spin–orbit coupling. We show how the transmission and the beam spin polarization critically depend on the incidence angle. The transmission halves when the incidence angle is greater than a limit angle and a significant spin polarization appears. On increasing the spin–orbit coupling one can obtain the modulation of the intensity and of the spin polarization of the output electronic current when the input current is unpolarized. Our analysis shows the possibility of realizing a spin-field-effect transistor based on the propagation of only one mode with the region with spin–orbit coupling, whereas the original Datta and Das device (1990 *Appl. Phys. Lett.* **56** 665) uses the spin precession that originates from the interference between two modes with orthogonal spin.

1. Introduction

One of the main goals of *spintronics* is the production and the control of spin-polarized currents [1, 2]. The attempts to realize the spin-field-effect transistor (spin-FET) proposed by Datta and Das [3], based on Rashba spin–orbit (SO) coupling [4], have been unsuccessful because of the difficulty of spin-polarized injection from a ferromagnetic metal into semiconductors [5]. Despite these obstacles several device setups based on the Rashba spin precession have been proposed [6–10]. Pala *et al* [11] have demonstrated the feasibility of a Datta and Das transistor with an all-semiconductor hybrid structure in which the charge carriers are the holes. A controlled source of spin-polarized electrons based on a mesoscopic equivalent

[1] Present address: Institut für Theoretische Physik, Universität Regensburg, D-93040, Germany.

of an optical polarizing beam splitter has been proposed [12]. Adiabatic pumping of spin in the presence of a fluctuating electric field, without ferromagnets, has been discussed [13]. Finally, Schliemann *et al* [14] have studied a spin-FET in which the electrons are subjected both to Rashba and Dresselhaus SO interaction [15]. They show that the balance of the interaction strengths gives rise to a decoupling of the spin-state and the momentum direction that allows a non-ballistic spin-FET.

In this paper we present the study of a hybrid system based on Rashba SO coupling without ferromagnetic contacts. We show that electrons injected unpolarized from a source are extracted with a partial spin polarization into a non-ferromagnetic drain. The electrons of a two-dimensional electron gas are injected at an out of normal incidence angle and the spin-FET operates by means of the spin-double refraction that appears at the interface between a region without SO coupling and a region where the SO coupling is present [16]. The use of spin-double refraction to produce and control spin-polarized current by means of the appearance of a limit angle for the refraction has also recently been proposed by [17] in a system complementary to ours: spin-unpolarized electrons from a Rashba source traverse a region with a lower SO coupling and are collected by a drain with a stronger Rashba coupling. In our case the strength of the SO coupling in the source and in the drain is zero. The source and the drain could be realized by using n^+-semiconductors. Our model uses an abrupt interface, but a smooth Rashba field should not change the effects of the spin-double refraction as the WKB approximation of [17] shows. The novel feature of our setup is the transmission double step shown in figure 2, that is accompanied by the appearance of a spin polarization. We stress that a modulation of the output current can be obtained with a spin-unpolarized input current, whereas in the original Datta and Das [3] proposal the current oscillation stems from the difference of phase accumulated along a path in the Rashba region by the two spin propagating modes. In our system the current modulation and the spin polarization appear when *only one mode* propagates through the Rashba barrier.

We take into account the phase averaging due to the thermal broadening that tends to wash out the effect of the multiple scattering against the two interfaces. We show how the resonances that appear when the electronic beam hits the interface with an angle greater than the first limit angle, when only one mode traverses the barrier, remain when the temperature is increased. On the other hand, the more rapid Fabry–Perot oscillation, with rapid changes of the transmission, due to the propagation of both the modes at low incidence angles are cancelled. The thermal average preserves the halving of the transmission strictly related to the appearance of the spin polarization, so that these features do not follow from the multiple scattering against the two interfaces.

2. Scattering against a region with SO coupling

Let us consider a two-dimensional electron gas (2DEG) filling the plane (x, z). A stripe, where the Rashba SO coupling is present, divides the plane into three regions, as in figure 1. In the inner region R $(0 < x < L)$ the Rashba SO coupling term is

$$\mathcal{H}_{\rm SO} = \frac{\hbar k_0}{m}(\vec{\sigma} \times \vec{p}) \cdot \hat{y} \tag{1}$$

where k_0 is the SO coupling constant, $\vec{\sigma}$ is the vector of Pauli matrices, $\vec{p}$ the momentum and m the electron mass. The strength of the SO coupling can be tuned by external gate voltages, as has been experimentally demonstrated [18–20]. In the outer regions NR $(x < 0$ and $x > L)$ there is no SO coupling $(k_0 = 0)$.

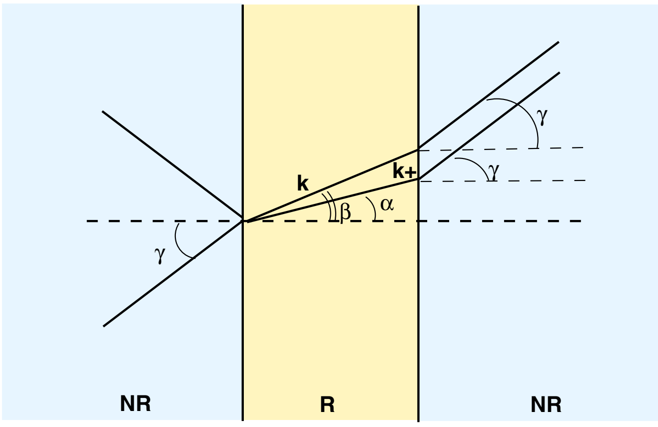

Figure 1. Schematic illustration of the proposed devices. The two-dimensional electron gas is divided into three regions. In the central region a Rashba spin–orbit coupling is present.

(This figure is in colour only in the electronic version)

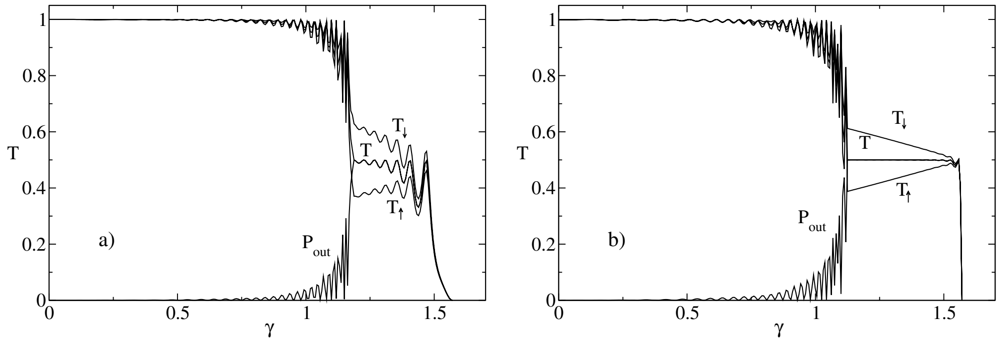

Figure 2. The transmission coefficients $T_{\downarrow}(\gamma)$, $T(\gamma)$, $T_{\uparrow}(\gamma)$ as functions of the incidence angle γ (in radians) at two values of the offset. The length L is 283 nm. Panel (a) shows the 1/2 height resonances, where $k_0/k = 0.05$ and $u_1/k^2 = 0.05$. The offset in panel (b) is $2k_0/k$ with the largest and the flattest low step obtainable, here $k_0/k = 0.05$, $u_1/k^2 = 0.1$ and $u/k = 0$.

Within the R zone there are two spin-split bands $E_{\pm}(k')$

$$E_{\pm}\left(k'\right) = \frac{\hbar^2}{2m}\left(k'^2 \pm 2k_0k'\right) \tag{2}$$

where $k' = \sqrt{k_x'^2 + k_z'^2}$ is the wavevector. The SO interaction can be viewed as due to a magnetic field parallel to the plane and orthogonal to the wavevector $\vec{k}'$. This magnetic field couples with the spin-magnetic moment and aligns the spin along the direction orthogonal to $\vec{k}'$ [21]. If $\vec{k}'$ is directed along x then the signs + and − indicate the 'spin up' and 'spin down' states in the z direction.

The spin-split bands may be shifted by applying an offset gate voltage V_{off} with respect to the source and drain bands $\hbar^2k^2/2m$. The energy bands (2) can be recast in the following form

$$E_\pm\left(k'\right)=\frac{\hbar^2}{2m}\left(k'^2\pm 2k_0k'\right)+eV_{\rm off}=\frac{\hbar^2}{2m}k^2$$
$$k'=\sqrt{k^2-u_1+k_0^2}\mp k_0=k_\pm \tag{3}$$
$$u_1=\frac{2meV_{\rm off}}{\hbar^2}.$$

The electron motion within the hybrid NR–R–NR system is supposed as ballistic and within the Landauer–Büttiker regime [22].

A single NR–R interface has a transmission coefficient dependent on the injection angle γ and on the incident spin state $|\delta\rangle=\cos\delta|\uparrow\rangle+\sin\delta|\downarrow\rangle$ because the Rashba effect gives rise to double refraction at the interface with two orthogonal spin polarizations that simultaneously propagate within the R zone only when $\gamma\neq 0$ [16] (out of the normal incidence). We have already analysed the case of a single NR–R interface [16] and, in this configuration, we have shown that the sum over all the injection angles reduces, but does not cancel, the spin-double refraction effect.

Our aim is to study the conductance of the NR–R–NR system in terms of the double interface transmission coefficient $T(\delta,\gamma)$.

In the $x<0$ region we have an incident and a reflected wave

$$\begin{pmatrix}\cos\delta\\ \sin\delta\end{pmatrix}{\rm e}^{{\rm i}k(x\cos\gamma+z\sin\gamma)}+\begin{pmatrix}r_\uparrow\\ r_\downarrow\end{pmatrix}{\rm e}^{{\rm i}k(-x\cos\gamma+z\sin\gamma)};$$

in the R region $(0<x<L)$ we have two propagating and two counterpropagating waves

$$\begin{pmatrix}\cos\alpha/2\\ -\sin\alpha/2\end{pmatrix}t_+{\rm e}^{{\rm i}k_+(x\cos\alpha+z\sin\alpha)}+\begin{pmatrix}\sin\beta/2\\ \cos\beta/2\end{pmatrix}t_-{\rm e}^{{\rm i}k_-(x\cos\beta+z\sin\beta)}$$
$$\begin{pmatrix}\sin\alpha/2\\ -\cos\alpha/2\end{pmatrix}r_+{\rm e}^{{\rm i}k_+(-x\cos\alpha+z\sin\alpha)}+\begin{pmatrix}\cos\beta/2\\ \sin\beta/2\end{pmatrix}r_-{\rm e}^{{\rm i}k_-(-x\cos\beta+z\sin\beta)};$$

and, finally, the transmitted wave for $x>L$ is

$$\begin{pmatrix}t_\uparrow\\ t_\downarrow\end{pmatrix}{\rm e}^{{\rm i}k(x\cos\gamma+z\sin\gamma)}.$$

The k_z parallel momentum conservation fixes the angular α and β directions of $\vec{k}'$

$$\alpha=\arcsin\frac{k\sin\gamma}{k_+}\qquad\text{and}\qquad\beta=\arcsin\frac{k\sin\gamma}{k_-}.$$

The modes (+) and (−) have the limit angles γ_0 and γ_1 respectively:

$$\gamma_0=\arcsin\frac{k_+}{k}\qquad\text{and}\qquad\gamma_1=\arcsin\frac{k_-}{k}, \tag{4}$$

that is, when γ exceeds γ_0 or γ_1 the corresponding mode becomes a decaying wave. The spinors of the wavefunction ψ for $0<x<L$ are independent of δ. In contrast, the spinors of the reflected and the transmitted wave depend on δ. In the inner region R the four amplitudes t_+, t_-, r_+, r_- vary with δ. The single NR–R interface is described by the Hamiltonian

$$\mathcal{H}_{\rm NR-R}=\vec{p}\frac{1}{2m(x)}\vec{p}+\frac{k_0(x)m(x)}{\hbar^2}\left(\sigma_zp_x-\sigma_xp_z\right)-{\rm i}\sigma_z\frac{1}{2}\frac{\partial k_0(x)}{\partial x}+u\delta(x). \tag{5}$$

We assume that the mass and the strength of SO coupling are piecewise constant:

$$\frac{1}{m}(x)=\frac{\vartheta(-x)}{m_{\rm NR}}+\frac{\vartheta(x)}{m_{\rm R}}$$
$$k_0(x)=k_0\vartheta(x), \tag{6}$$

where $\vartheta(x)$ is the step function. To have a model as simple as possible, we assume that the electron effective mass in the NR region $m_{\rm NR}$ and the electron effective mass in the R $m_{\rm R}$ region are equal. The third term in (5) is needed to get a Hermitian operator $\mathcal{H}_{\rm NR-R}$. The fourth term regulates the transparency of the interface and describes insulating barriers separating the semiconductors. The matching conditions at $x = 0$ and L

$$\begin{aligned}&\psi\,(0+) - \psi\,(0-) = 0\\ &\psi\,(L+) - \psi\,(L-) = 0\\ &\partial_x\psi\,(0+) - \partial_x\psi\,(0-) = (u - \mathrm{i}k_0)\,\psi\,(0)\\ &\partial_x\psi\,(L+) - \partial_x\psi\,(L-) = (u + \mathrm{i}k_0)\,\psi\,(L)\end{aligned}$$

provide a linear system for the eight quantities $r_\uparrow, r_\downarrow, t_\uparrow, t_\downarrow, t_+, t_-, r_+, r_-$. The R region behaves as a resonant cavity whose action can be reinforced by the couple of additional Dirac-delta potentials. The strength u of those controls the interface's transparency.

To avoid ferromagnetic leads we consider unpolarized electrons injected into the NR–R–NR system. The unpolarized statistical mixture at $x = 0$

$$\rho_{\rm in} = \tfrac{1}{2}\,|\uparrow\rangle\,\langle\uparrow| + \tfrac{1}{2}\,|\downarrow\rangle\,\langle\downarrow|$$

becomes the density matrix $\rho_{\rm out}$ at $x = L$:

$$\rho_{\rm out} = \tfrac{1}{2}T_\uparrow\,|1\rangle\,\langle 1| + \tfrac{1}{2}T_\downarrow\,|2\rangle\,\langle 2| \qquad (7)$$

where $T_\uparrow = \left|t_{\uparrow\uparrow}\right|^2 + \left|t_{\downarrow\uparrow}\right|^2$ is the coefficient for the incoming spin up state and $T_\downarrow = \left|t_{\uparrow\downarrow}\right|^2 + \left|t_{\downarrow\downarrow}\right|^2$ is that for the incoming spin down state[2]. The spinors in the operator (7) are

$$|1\rangle = \frac{1}{\sqrt{T_\uparrow}}\begin{pmatrix} t_{\uparrow\uparrow}\\ t_{\downarrow\uparrow}\end{pmatrix} \qquad \text{and} \qquad |2\rangle = \frac{1}{\sqrt{T_\downarrow}}\begin{pmatrix} t_{\uparrow\downarrow}\\ t_{\downarrow\downarrow}\end{pmatrix} \qquad (8)$$

corresponding to input spin up and down respectively. The transmission coefficient of the unpolarized electrons is

$$T = \left(T_\uparrow + T_\downarrow\right)/2.$$

We note that $\rho_{\rm out}$ can be represented in terms of the output polarization $\vec{P}$ as

$$\rho_{\rm out}\,(\gamma) = \tfrac{1}{2}(\mathbf{1} + \vec{P}\,(\gamma)\cdot\vec{\sigma}) \qquad (9)$$

where $\vec{P}$ is the average of $\vec{\sigma}$:

$$\vec{P} = \langle\vec{\sigma}\rangle = \mathrm{Tr}\left[\rho_{\rm out}\vec{\sigma}\right].$$

The modulus of $\vec{P}$ gives the degree of polarization in the output. A simple calculation shows that the modulus of the polarization $P_\uparrow$ of the spinor $\sqrt{T_\uparrow}\,|1\rangle$ is $P_\uparrow \equiv T_\uparrow$, whereas the modulus of the polarization $P_\downarrow$ of $\sqrt{T_\downarrow}\,|2\rangle$ is $P_\downarrow \equiv T_\downarrow$. Finally, when the input state is unpolarized the output state is partially polarized. In particular, for $\gamma > \gamma_0$ we get

$$|\vec{P}_{\rm out}| = \tfrac{1}{2}\left(T_\uparrow + T_\downarrow\right) = T \qquad \text{for } \gamma > \gamma_0 \qquad (10)$$

since $|\langle 1|2\rangle|$ goes very quickly to 1. In contrast, when the incidence angle γ is lower than γ_0, $|\vec{P}_{\rm out}| < T$ and the polarization vanishes when γ goes to zero.

Finally, for $\gamma > \gamma_0$ some resonances appear (see figure 2) for which

$$\begin{aligned}R_\uparrow &= T_\downarrow\\ R_\downarrow &= T_\uparrow,\end{aligned}$$

[2] The first arrow in the label of the transmitted amplitudes represents the output spin, whereas the second arrow indicates the input spin.

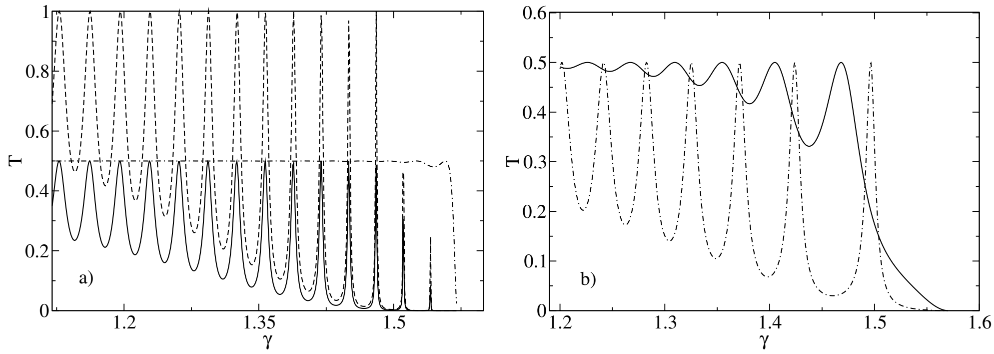

Figure 3. Panel (a): The transmission coefficient for unpolarized electrons as a function of the injection angle. The solid curve is for $u_1/k^2 = 0.1$, $u/k = 0.4$ and $k_0/k = 0.05$, the dashed curve is for $u_1/k^2 = 0$, $u/k = 0.4$ and $k_0/k = 0$, and finally the dotted–dashed curve is for $u_1/k^2 = 0.1$, $u/k = 0.4$ and $k_0/k = 0.05$. Panel (b): The transmission coefficient for unpolarized electrons as a function of the injection angle. The solid curve is for $u_1/k^2 = 0.05$, $u/k = 0.0$ and $k_0/k = 0.05$, and the dotted–dashed curve is for $u_1/k^2 = 0.05$, $u/k = 0.4$ and $k_0/k = 0.05$.

where $R_\uparrow$ and $R_\downarrow$ are the reflection coefficients with an incident spin up or down. For the unpolarized statistical mixture the flux conservation implies that at the resonances

$$T = \tfrac{1}{2}\left(T_\uparrow + T_\downarrow\right) = R = \tfrac{1}{2}\left(R_\uparrow + R_\downarrow\right) = \tfrac{1}{2}.$$

The calculated transmission coefficients for unpolarized ($T(\gamma)$) and polarized ($T_\downarrow(\gamma)$, $T_\uparrow(\gamma)$) injected electrons are shown in figure 2 with realistic parameters [18–20]. For the inverted $In_{0.53}Ga_{0.47}As/In_{0.52}Al_{0.48}As$ heterostructure the value of the Fermi wavevector is $k = 3.53 \times 10^6$ cm^{-1}, and the effective mass is $m = 0.05\, m_e$, whereas the strength of the SO k_0 ranges from $0.01k$ to $0.05k$. The main feature of $T_\downarrow$, T, $T_\uparrow$ is the double step that originates from the spin-double refraction. When γ goes over γ_0 only the wave $(-)$ can reach the second interface and the transmission coefficients tend to halve themselves. Panel (a) of figure 2 shows that, when $\gamma > \gamma_0$, the resonances of the unpolarized transmission T have height $1/2$. At the offset $u_1/k^2 = 2k_0/k$ a limit angle γ_1 also appears for the wave $(-)$. On increasing the offset to higher values both the limit angles γ_0 and γ_1 tend to zero. At the offset $2k_0k$ the second step of the transmission becomes almost perfectly squared, as the panel (b) of figure 2 shows. At this optimum value, we have $k_- \equiv k$ and $\beta \equiv \gamma$: the mode $(-)$ is no longer refracted. With $u = 0$ and γ greater than γ_0 the resonances within the cavity disappear.

Since the output spin polarization of the electrons entering with spin up or down coincides at any angle γ with $T_\uparrow$ or $T_\downarrow$ then the crossing of the R zone depolarizes the electrons. The polarization P_{out} of the electrons entering unpolarized is equal to T only for $\gamma > \gamma_0$, and for $\gamma < \gamma_0$ it tends to zero for $\gamma \to 0$: the crossing of the R zone gives rise to a spin polarization that is absent at normal incidence. At the optimum value of the offset $u_1 = 2kk_0$ and for $\gamma > \gamma_0$, P_{out} is independent of the incidence angle. We note that this feature is robust with respect to few elastic scattering events that conserve k but change its direction. This behaviour recalls the non-ballistic spin-FET proposed by Schliemann *et al* [14].

Is is interesting to do an analysis on the proper modes of the Rashba region. Figure 3 shows the transmission as a function of the injection angle for $\gamma > \gamma_0$ and several values of the parameters. In panel (a) of figure 3 the dashed curve corresponds to the proper mode of the cavity without SO coupling ($u_1/k^2 = 0$, $u/k = 0.4$ and $k_0/k = 0$). If we now turn on the SO coupling and choose the offset to the optimum value $u_1 = 2k_0k$ (solid curve—$u_1/k^2 = 0$, $u/k = 0.4$ and $k_0/k = 0.05$) we observe the halving of the transmission maxima but those

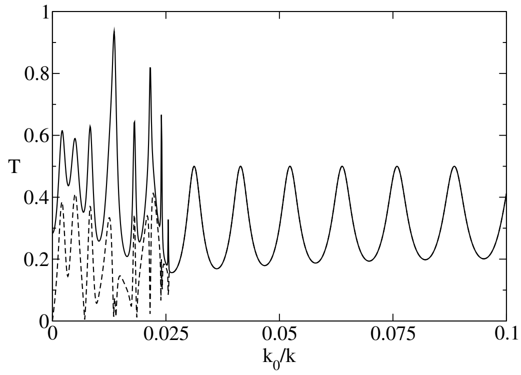

Figure 4. The transmission coefficient for unpolarized electrons when $\gamma = 1.25$. The threshold $\overline{k_0}$ is $0.025k$. The dotted curve gives the output spin polarization, $L = 283$ nm and we have put $u/k = 0.4$ to enhance the resonances in the low step of the transmission.

preserve the proper modes of the cavity. The proper modes of the cavity are washed out for a perfectly transparent cavity at the optimum offset (dotted–dashed curve—$u_1/k^2 = 0.1$, $u/k = 0$ and $k_0/k = 0.05$). In the last case the flatness of the transmission coefficient (and of the polarization vector) is independent by effects related to multiple reflections inside the cavity. In panel (b) of figure 3 are reported similar results with the offset to a value lower than the optimum one, demonstrating how a perfectly transparent barrier ($u = 0$) has proper modes due only to SO coupling and how these modes modify when u increases.

We stress that the dependence of the limit angle γ_0 on the SO strength k_0 suggests the possibility of building up a spin-FET operating on spin-unpolarized electrons injected in the R region. The electrons emerge in the NR drain region partially polarized with a polarization controlled by a gate electrode via the SO interaction. There is an SO strength $\overline{k_0}$ at which $\gamma = \gamma_0$. Figure 4 shows that the transmission coefficient exhibits irregular Fabry–Perot oscillations below $\overline{k_0}$, whereas for $k_0 > \overline{k_0}$ the oscillations become regular with maxima equal to $1/2$. The threshold $\overline{k_0}$ is determined by the offset

$$u_1/k^2 = 2\overline{k_0}/k,$$

for which γ_0 goes over γ and the wave (+) propagation ceases. When $k_0 > \overline{k_0}$ the polarization of electrons in the NR drain P_{out} is equal to T, as we have seen before. We get a source of a spin-polarized current controlling k_0 with a gate.

We notice that Mireles and Kirczenow [23] have studied the scattering against a finite Rashba region within a quantum wire. They show that, injecting spin up electrons, the ballistic spin conductance oscillates varying the SO coupling strength, and they claim that these results may be of relevance for the implementation of a quasi-one-dimensional spin transistor device. We have shown that a ballistic conductance oscillation with k_0 also appears without lateral confinement and without a ferromagnetic source and drain, that is by handling spin-unpolarized electrons.

Another issue that deserves some attention is the inclusion of the linear term due to Dresselhaus spin–orbit coupling [15]. There is recent experimental evidence [24] that the Dresselhaus coupling in some heterostructures can be of the same order of the Rashba coupling, up to one half of the Rashba strength. Some preliminary results for a single interface with a Rashba zone indicate that, even in the less favourable case of normal incidence, the addition of a Dresselhaus term everywhere in the 2DEG plane gives different transmissions for the two orthogonal incident spin states. In our opinion the further inclusion of the Dresselhaus spin–orbit coupling should even enhance the polarization effects that we have found with only the Rashba term.

3. Phase averaging due to the thermal broadening

Now we want to take into account the smoothing effect of the Fermi surface due to finite temperatures. Supposing that we are in the linear response regime, we have for the current I

$$I = G(E_F)\frac{\mu_1 - \mu_2}{e}$$

$\mu_1 - \mu_2$ being the applied bias and $G(E_F)$ the conductance ($\mu_1 - \mu_2 \ll E_F$). For a ballistic conductor [25]

$$G(E_F) = \frac{2e^2}{h}\int T(E)F_T(E - E_F)\,dE$$

where $F_T(E - E_F)$ is the thermal broadening function

$$F_T(E - E_F) = -\frac{d}{dE}\frac{1}{\exp[(E - E_F)/k_B\overline{T}] + 1} = \frac{1}{4k_B\overline{T}}\,\mathrm{sech}^2\left(\frac{E}{2k_B\overline{T}}\right)$$

$\overline{T}$ being the temperature. The thermal average of the transmission is

$$\langle T\rangle_{th} = \int T(E)F_T(E - E_F)\,dE.$$

If we approximate the Fermi–Dirac distribution with the ramp

$$\begin{array}{ll} 1 & E < E_F - 2k_B\overline{T} \\ \frac{1}{2} - (E - E_F)/4k_B\overline{T} & E_F - 2k_B\overline{T} < E < E_F + 2k_B\overline{T} \\ 0 & E > E_F + 2k_B\overline{T} \end{array}$$

we get

$$\langle T\rangle_{th} = \frac{1}{2\Delta k}\int_{k_F-\Delta k}^{k_F+\Delta k} T(k)\,dk \tag{11}$$

where we assume that

$$\Delta k = \frac{k_B\overline{T}}{E_F}k_F \ll k_F.$$

With a Fermi energy $E_F = 14$ meV, and $\overline{T} = 3$ K we have $\Delta k/k_F = 0.018$, and in the following we choose $\Delta k/k_F = 0.03$ corresponding to a temperature of 5 K. We start by considering the thermal average of the transmissions. In figure 5 we show the averaged transmission for various values of the offset. In panel (a) of figure 5 the offset is $u_1/k^2 = 0.05$, and few resonances appear when γ is larger than γ_0; on increasing the temperature up to 5 K the rapid oscillations of the transmission below γ_0 are almost completely cancelled, whereas the resonances of the (−) mode are still well defined in the averaged transmission. In panel (b) of figure 5 the offset is chosen at the optimum value $u_1/k^2 = 2k_0/k = 0.1$. We observe again an almost perfectly squared transmission step among γ_0 and $\pi/2$, whereas below γ_0 the rapid Fabry–Perot oscillations are washed out. The transmission steps for a larger offset $u_1/k^2 = 0.2$ at 0 K and at 5 K are compared in panels (c) and (d) of figure 5. In this case the transmission oscillations are cancelled at any incidence angle but the double step structure survives.

The thermal averaging was also performed on the polarization vector, and figure 6 shows the average calculated with equation (11) of the modulus of the polarization vector and of its

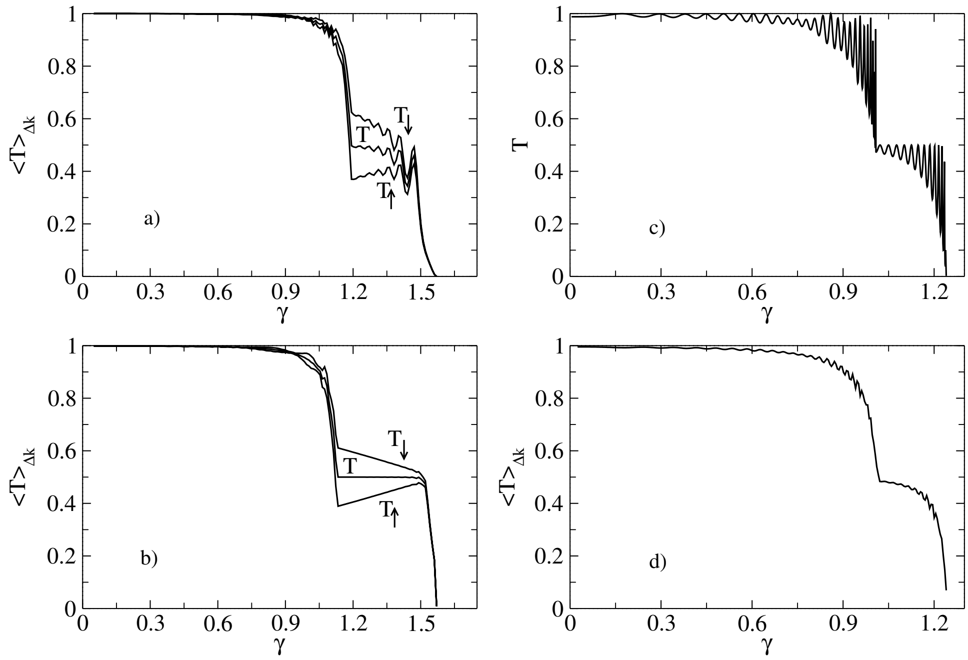

Figure 5. Panel (a): Thermally averaged transmission coefficient for unpolarized electrons as a function of the injection angle. The curves are relative to $u_1/k^2 = 0.05$, $u/k = 0$ and $k_0/k = 0.05$. The thermal average corresponds to a temperature of 5 K. Panel (b): As in panel (a), but with $u_1/k^2 = 0.1$, $u/k = 0$ and $k_0/k = 0.05$. The thermal average corresponds to a temperature of 5 K. Panel (c): Transmission coefficient at 0 K for unpolarized electrons as a function of the injection angle with $u_1/k^2 = 0.2$, $u/k = 0$ and $k_0/k = 0.05$. Panel (d): Thermally averaged transmission coefficient for unpolarized electrons as a function of the injection angle. The curve is relative to $u_1/k^2 = 0.2$, $u/k = 0$ and $k_0/k = 0.05$. The thermal average corresponds to a temperature of 5 K.

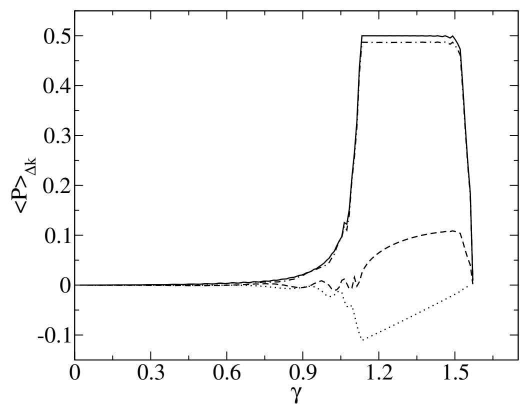

Figure 6. Thermally averaged polarization as a function of the injection angle. The solid curve is the modulus of the polarization vector, the dashed–dotted curve corresponds to $\langle\sigma_x\rangle$, the dashed curve corresponds to $\langle\sigma_y\rangle$ and the dotted curve corresponds to $\langle\sigma_z\rangle$. The curves are evaluated for $u_1/k^2 = 0.1$, $u/k = 0$ and $k_0/k = 0.05$. The thermal average corresponds to a temperature of 5 K.

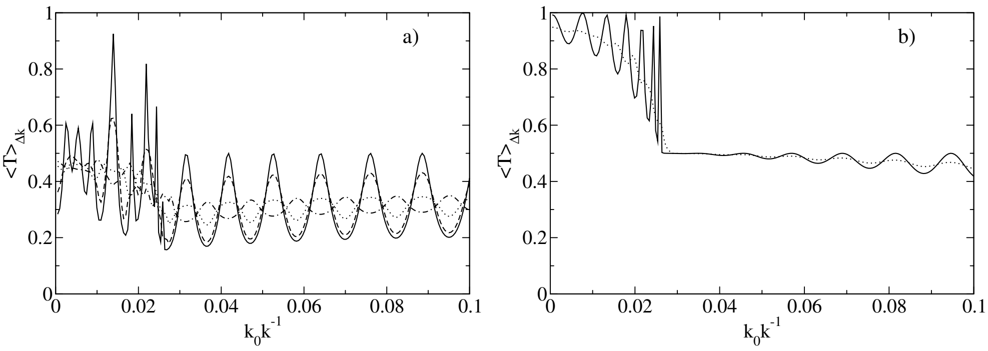

Figure 7. The thermally averaged transmission coefficient for unpolarized electrons when $\gamma = 1.25$ as a function of the spin–orbit coupling. The threshold $\overline{k_0}$ is $0.025k$. Panel (a): The solid curve corresponds to zero temperature, the dashed curve to a temperature of 3 K, the dotted curve to a temperature of 5 K and the dashed–dotted to a temperature of 8 K. Panel (b): The thermally averaged transmission coefficient for unpolarized electrons when $\gamma = 1.25$ as a function of the spin–orbit coupling at 5 K (solid curve) and 8 K (dotted curve), with perfectly transparent interfaces ($u = 0$).

three components. The offset is at the optimum value and the output spin polarization tends to be nearly orthogonal to the interfaces as one would expect, because $\vec{k}_-$ has a small component in the x direction and the spin and the momentum are orthogonal to each other.

Figure 7 shows the thermal average of the transmission of unpolarized electrons as a function of the SO strength with the same parameters as figure 4, where the transmission has been calculated at 0 K. Therefore we judge that an increase of a few kelvins does not cancel the modulation effect.

4. Conclusions

We have shown that the spin-double refraction in an NR–R–NR system allows both the current modulation and the polarization of spin-unpolarized injected electrons. Furthermore, the existence of limit angles for the propagation within the structure involves the halving of the transmission, and this could be searched for as a sign of the double refraction phenomenon. As regards the feasibility of the studied hybrid system, we stress that our calculations use realistic parameter values for the Rashba SO coupling [18]. We think that the physics of spin-double refraction and its use to produce and control spin-polarized currents should be within present experimental investigations. We propose that the injection of an electron beam with an incidence angle on a Rashba barrier greater than the limit angle gives an output current modulated by the SO strength. Our proposal is different from the original one of Datta and Das [3] in which the current modulation stems from the interference of both the modes (+) and (–); that is, from the precession within the Rashba region. Instead we propose to use the spin rotation that appears when an electron beam goes through the interfaces with a incident angle γ out of the normal. Such an angle could be realized by using an adiabatic quantum point contact as a source in which the constriction axis forms the angle γ with the NR–R interface.

Acknowledgments

We gratefully acknowledge helpful discussions with I D'Amico, D Frustaglia and M Governale.

Appendix. Output spin polarization evaluation

In this appendix we give the proof of the relation (10). In the general case, when we work with density matrix operator

$$\rho = \sum_m |m\rangle p_m \langle m|,$$

the average value of the observable A is the trace of ρA:

$$\langle A\rangle = \mathrm{Tr}\,[\rho A]\,,$$

that in terms of the density matrix elements is equal to

$$\mathrm{Tr}\,[\rho A] = \sum_m p_m(|m\rangle\langle m|A) = \sum_m p_m\langle m|A|m\rangle.$$

In the present case the density matrix operator has been defined in equation (7) with the components (8). The averaged value of the modulus of the polarization is defined by

$$|\vec{P}_{\mathrm{out}}| = \sqrt{\langle\sigma_x\rangle^2 + \langle\sigma_y\rangle^2 + \langle\sigma_z\rangle^2}. \tag{A.1}$$

Using the density matrix operator (7) we have that

$$\begin{aligned}\langle\sigma_x\rangle &= \tfrac{1}{2}\left(t^*_{\uparrow\uparrow}t_{\downarrow\uparrow} + t^*_{\downarrow\uparrow}t_{\uparrow\uparrow} + t^*_{\uparrow\downarrow}t_{\downarrow\downarrow} + t^*_{\downarrow\downarrow}t_{\uparrow\downarrow}\right)\\ \langle\sigma_y\rangle &= -\frac{\mathrm{i}}{2}\left(t^*_{\uparrow\uparrow}t_{\downarrow\uparrow} - t^*_{\downarrow\uparrow}t_{\uparrow\uparrow} + t^*_{\uparrow\downarrow}t_{\downarrow\downarrow} - t^*_{\downarrow\downarrow}t_{\uparrow\downarrow}\right)\\ \langle\sigma_z\rangle &= \tfrac{1}{2}(|t_{\uparrow\uparrow}|^2 - |t_{\downarrow\uparrow}|^2 + |t_{\uparrow\downarrow}|^2 - |t_{\downarrow\downarrow}|^2).\end{aligned} \tag{A.2}$$

Substituting the relations (A.2) into (A.1) we have that

$$\begin{aligned}|\vec{P}_{\mathrm{out}}|^2 = \tfrac{1}{4}[&|t_{\uparrow\uparrow}|^4 + |t_{\downarrow\uparrow}|^4 + |t_{\uparrow\downarrow}|^4 + |t_{\downarrow\downarrow}|^4 + 2(|t_{\uparrow\uparrow}|^2|t_{\downarrow\uparrow}|^2 + |t_{\uparrow\uparrow}|^2|t_{\uparrow\downarrow}|^2\\ &- |t_{\uparrow\downarrow}|^2|t_{\downarrow\uparrow}|^2 + |t_{\downarrow\downarrow}|^2|t_{\downarrow\uparrow}|^2 + |t_{\downarrow\downarrow}|^2|t_{\uparrow\downarrow}|^2 - |t_{\downarrow\downarrow}|^2|t_{\uparrow\uparrow}|^2\\ &+ 2t_{\downarrow\downarrow}t_{\uparrow\uparrow}t^*_{\downarrow\uparrow}t^*_{\uparrow\downarrow} + 2t^*_{\downarrow\downarrow}t^*_{\uparrow\uparrow}t_{\downarrow\uparrow}t_{\uparrow\downarrow})].\end{aligned} \tag{A.3}$$

When the injection angle γ approaches zero, we have that the system does not flip the spin; that is, $t_{\uparrow\downarrow} = t_{\downarrow\uparrow} = 0$ so that

$$|\vec{P}_{\mathrm{out}}| = \tfrac{1}{2}||t_{\uparrow\uparrow}|^2 - |t_{\downarrow\downarrow}|^2|; \tag{A.4}$$

that is, in the case of injection of unpolarized electrons the output polarization is zero.

We note that in the R zone the spin states of the (+) and (−) modes given by the spinors $|1\rangle$ and $|2\rangle$ are conserved [16]. The output spin state is strictly determined by the transmitted amplitudes of the interfaces. The interference between the (+) and (−) modes when both are present ($\gamma < \gamma_0$) makes the polarization different from the transmission, as equation (A.4) shows. When $\gamma > \gamma_0$ only the (−) mode survives in the R zone. This is demonstrated by the fact that the inner product between the state $|1\rangle$ and $|2\rangle$ goes to one:

$$|\langle 1|2\rangle| = 1 \qquad \text{for } \gamma > \gamma_0;$$

this means that the two wavefunctions, for $\gamma > \gamma_0$, differ for a phase factor

$$|1\rangle = \mathrm{e}^{-\mathrm{i}\phi}\,|2\rangle \rightarrow \frac{1}{\sqrt{T_\uparrow}}\begin{pmatrix}t_{\uparrow\uparrow}\\ t_{\downarrow\uparrow}\end{pmatrix} = \mathrm{e}^{-\mathrm{i}\phi}\frac{1}{\sqrt{T_\downarrow}}\begin{pmatrix}t_{\uparrow\downarrow}\\ t_{\downarrow\downarrow}\end{pmatrix}. \tag{A.5}$$

Using the previous relation we can express $t_{\uparrow\downarrow}$ and $t_{\downarrow\uparrow}$ as a function of $t_{\uparrow\uparrow}$ and $t_{\downarrow\downarrow}$:

$$t_{\downarrow\uparrow} = \mathrm{e}^{\mathrm{i}\phi}\sqrt{\frac{T_\downarrow}{T_\uparrow}}t_{\uparrow\uparrow} \qquad \text{and} \qquad t_{\uparrow\downarrow} = \mathrm{e}^{-\mathrm{i}\phi}\sqrt{\frac{T_\uparrow}{T_\downarrow}}t_{\downarrow\downarrow}. \tag{A.6}$$

Substituting those expressions in (A.3), we have

$$|\vec{P}_{\text{out}}| = \frac{1}{2}\left[|t_{\uparrow\uparrow}|^2 + |t_{\downarrow\downarrow}|^2 + \frac{T_{\uparrow}^2}{T_{\downarrow}^2}|t_{\downarrow\downarrow}|^2 + \frac{T_{\downarrow}^2}{T_{\uparrow}^2}|t_{\uparrow\uparrow}|^2\right] \tag{A.7}$$

and using the relations (A.6) this is equivalent to

$$|\vec{P}_{\text{out}}| = \frac{1}{2}\left[|t_{\uparrow\uparrow}|^2 + |t_{\downarrow\downarrow}|^2 + |t_{\uparrow\downarrow}|^2 + |t_{\downarrow\uparrow}|^2\right] = \frac{T_{\uparrow} + T_{\downarrow}}{2} = T. \tag{A.8}$$

References

[1] Awschalom D D, Loss D and Samarth N (ed) 2002 *Semiconductor Spintronics and Quantum Computation* (Berlin: Springer)
[2] Žutíc I, Fabian J and Das Sarma S 2004 *Rev. Mod. Phys.* **76** 323
[3] Datta S and Das B 1990 *Appl. Phys. Lett.* **56** 665
[4] Rashba E I 1960 *Fiz. Tverd. Tela* **2** 1234
Rashba E I 1960 *Sov. Phys.—Solid State* **2** 1109 (Engl. Transl.)
[5] Schmidt G, Ferrand D, Molenkamp L W, Filip A T and Van Wees B J 2000 *Phys. Rev.* B **62** 4790(R)
[6] Kiselev A A and Kim K W 2001 *Appl. Phys. Lett* **78** 775
[7] Koga T, Nitta J, Takayanagi H and Datta S 2002 *Phys. Rev. Lett.* **88** 126601
[8] Egnes J C, Burkard G and Loss D 2002 *Phys. Rev. Lett.* **89** 176401
[9] Jiang Y and Jalil M B 2003 *J. Phys.: Condens. Matter* **15** L31
[10] Frustaglia D and Richter K 2004 *Phys. Rev.* B **69** 235310
[11] Pala M G, Governale M, König J and Zülicke U 2004 *Europhys. Lett.* **65** 850
[12] Ionicioiu R and D'Amico I 2003 *Phys. Rev.* B **67** 041307(R)
[13] Governale M, Taddei F and Fazio R 2003 *Phys. Rev.* B **68** 155324
[14] Schliemann J, Carlos Egues J and Loss D 2003 *Phys. Rev. Lett.* **90** 146801
[15] Dresselhaus G 1955 *Phys. Rev.* **100** 580
[16] Marigliano Ramaglia V, Bercioux D, Cataudella V, De Filippis G, Perroni C A and Ventriglia F 2003 *Eur. Phys. J.* B **36** 365
[17] Khodas M, Shekhter A and Finkel'stein A M 2004 *Phys. Rev. Lett.* **92** 086602
[18] Nitta J, Akazaki T, Takayanagi H and Enaki T 1997 *Phys. Rev. Lett.* **78** 1138
[19] Schäpers T, Engels J, Klocke T, Hollfelder M and Lüth H 1998 *J. Appl. Phys.* **83** 4324
[20] Grundler D 2000 *Phys. Rev. Lett.* **84** 6074
[21] Bychkov Y A and Rashba E I 1984 *J. Phys. C: Solid State Phys.* **17** 6039
[22] Ferry D K and Goodnick S M 1997 *Transport in Nanostructures* (Cambridge: Cambridge University Press)
[23] Mireles F and Kirczenow G 2001 *Phys. Rev.* B **64** 024426
[24] Ganichev S D, Bel'kov V V, Golub L E, Ivchenko E L, Schneider P, Giglberger S, Eroms J, De Boeck J, Borghs G, Wegscheider W, Weiss D and Prettl W 2004 *Phys. Rev. Lett.* **92** 256601
[25] Datta S 1995 *Electronic Transport in Mesoscopic Systems* (Cambridge: Cambridge University Press)